



## THIENOTHIOPHENE UNITS PROPERTIES ON THE CARBAZOLE-BASED POLYMERS FOR ORGANIC SOLAR CELL DEVICES

(Pencirian Unit Tienotiofen Dalam Polimer Berasaskan Karbazol Untuk Penggunaan Sel Solar Organik)

Mohd Sani Sarjadi<sup>1\*</sup>, Hunan Yi<sup>2</sup>, Ahmed Iraqi<sup>2</sup>, David G. Lidzey<sup>3</sup>

<sup>1</sup>Faculty of Science and Natural Resources,  
Universiti Malaysia Sabah, 88400 Kota Kinabalu, Sabah, Malaysia

<sup>2</sup>Department of Chemistry,  
University of Sheffield, Sheffield S3 7HF, UK

<sup>3</sup>Department of Physics & Astronomy,  
University of Sheffield, Hicks Building, Hounsfield Road, Sheffield S3 7RH, UK

\*Corresponding author: msani@ums.edu.my

Received: 9 December 2014; Accepted: 16 October 2015

### Abstract

The development of new polymers-based for application in plastic solar cells is attracting much research interest for their potential as a low-cost system for renewable energy generation. We report herewith a comparative study on three donor-acceptor carbazole-based copolymers containing thienothiophene moieties for application in organic photovoltaic (OPV) devices. The polymers were synthesised by Suzuki cross coupling, in order to investigate its suitability to enhance the polymer properties in photovoltaic cell. Morphological, spectroscopic and charge-transport measurements are used to investigate the influence of either the thienothiophene moieties on the structure and photophysical properties of the copolymer rationalise the solar cell characteristics. The optical band gap,  $E_g$  of polymers **P1**, **P2** and **P3** were 2.46 eV, 2.36 eV and 2.47 eV respectively. The photophysical properties of these polymers show that **P2** has the narrowest optical band gap due to the electrostatic interaction between the hydrogens at the 4-position on thienothiophene rings and the fluorine substituents on the neighbouring carbazole repeat units. These results are in agreement with the design procedures for the use of these materials in photovoltaic applications. We tentatively explain such differences on the basis of reduced molar absorbance and reduced charge-carrier mobility in the thienothiophene-based polymers.

**Keywords:** conjugated polymers, thienothiophene, Suzuki cross coupling, solar cells

### Abstrak

Pembangunan penggunaan polimer-berasaskan sel solar plastik baru menjadi tumpuan ramai penyelidik yang berminat kepada potensi sistem murah untuk generasi yang memperbaharui tenaga. Kami melaporkan kajian tiga ko-polimer penderma-penerima berasaskan-karbazol yang mengandungi tienotiofen untuk digunakan dalam sel fotovoltac organik (OPV). Polimer disintesis dengan kaedah pengganding silang Suzuki dengan kajian kesesuaiannya meningkatkan ciri-ciri polimer sel fotovoltac. Sifat morfologi, spektroskopik dan ukuran perpindahan-cas digunakan untuk mengkaji pengaruh persekitaran struktur tienotiofen dan sifat fotofizikal bagi kopolimer untuk mengetahui kesesuaian ciri-ciri bagi sel solar. Nilai jurang tenaga optikal,  $E_g$  bagi polimer P1, P2 dan P3 masing-masing adalah 2.46 eV, 2.36 eV dan 2.47 eV. Sifat fotofizikal **P2** menunjukkan nilai jurang tenaga optikal paling dekat kerana interaksi elektrostatik di antara hidrogen kedudukan-4 dalam struktur gelang tienotiofen dan unsur penukar ganti florin dalam unit berulang karbazol. Keputusan ini memenuhi prosedur bagi menggunakan bahan ini dalam aplikasi fotovoltac. Kami juga menerangkan perbezaan asas bagi penurunan molar penyerapan dan pembawa-cas di dalam polimer berstruktur asas-tienotiofen.

**Kata kunci:** polimer berkonjugat, tienotiofen, pengganding silang Suzuki, sel solar

### Introduction

The science and technology of conjugated polymers continues to be a vibrant and exciting research area nearly 30 years after the initial explosion of interest in these materials [1]. The materials may combine the processability and outstanding mechanical characteristics of polymers with the readily-tailored electrical, optical and magnetic properties of functional organic molecules [2, 3]. In the late 1970s and early 1980s the rediscovery of conjugated polymers like polyacetylene, polyaniline, polypyrrole and polythiophene ignited an intense investigation of the properties of these inherently conducting materials [4-6]. Conjugated polymers are organic macromolecules which consist of alternating single and double carbon-carbon bonds along the polymer chain, where the hybridization between 2s and 2p orbitals of carbon atom leads to three  $sp^2$  hybrid orbitals and  $p_z$  orbital which is perpendicular to other orbitals [1, 2, 7, 8].

In particular the potential use of these materials in light-emitting diodes (LEDs), field-effect transistors (FETs), photovoltaic cells (PV), and other opto-electronic devices has motivated the development of synthesis and processing methods of conjugated polymer materials with unique properties [6, 9, 10]. The device performance is critically dependent on the quality of the thin film of the conjugated polymer coating on these devices. Many applications for conjugated polymers rely on their facile and reversible electrochemistry, where the polymer can be oxidised and reduced with simultaneous change in properties [11]. The switchable properties are the basic of the application as transistors, sensors, re-chargeable batteries, solar cells, capacitors and even mechanical actuators.

In the 1980s, the concepts of polarons, bipolarons, and solitons were developed, in the context of both transport properties and optical properties [7, 12]. However, the photoconductivity properties of materials such as thienothiophene and selenium received the attention of researchers, not the photovoltaic properties [13-15]. During the past few years, researchers found the donor-acceptor system offers stable quinoid form of polymer, because the interactions between the two units will enhance the double bond between the units. Also, the zwitterions interaction between alternate units planarised the polymer structure and stabilized the reduced bandgap quinoid form [16]. The essential ideas about the nature of the unusual charge bearing species, and of the excited states of conjugated systems, have been discussed intensely over the past twenty years [5, 8, 17, 18] This discovery led to develop of polymer/fullerene (Donor/Acceptor) heterojunction photovoltaic devices. It is based on mixing the donor and acceptor to increase the interfacial area, therefore the efficiency of the devices [19-21] Other attempts were carried out to control the morphology of the active layer in devices for example disordered or ordered bulk heterojunction (BHJ) and molecular heterojunction [22].

Recently, however, there has been a refinement of these ideas, which enables a better understanding of certain features of the electronic structure of conjugated polymers. The rather short history of BHJ solar cells can be roughly divided into three phases from the perspective of the conjugated backbones of donor polymers. Phase one centered on poly(phenylene vinylene)s (PPV), such as poly[2-methoxy-5-(2'-ethylhexyloxy)-1,4-phenylenevinylene] (MEH-PPV) and poly[2-methoxy-5-(3',7'-dimethyloctyloxy)-1,4-phenylenevinylene] (MDMO-PPV) [23]. Therefore, in phase two, a smaller-band-gap polymer, regioregular poly(3-hexylthiophene) (rr-P3HT), was thoroughly investigated. P3HT-based BHJ devices provide a noticeably higher current density (over 10  $\text{mA}/\text{cm}^2$ ), attributed to its lower band gap (1.9 eV) as well as to its increased  $\pi$ -stacking and crystallinity which yields a higher hole mobility [24-27]. However, due to the interplay of polymer properties such as energy levels and band gap and their correlation with  $V_{oc}$  and  $J_{sc}$ , highest  $V_{oc}$  and highest  $J_{sc}$  cannot be concurrently obtained [21].

In this work a detailed physical study is undertaken to explore the optical properties of these three conjugated polymers in order to understand the thienothiophene impact.

## Materials and Methods

### Materials

Materials used for the preparation of monomers were purchased from the commercial suppliers and used as received unless otherwise stated. All solvent used for the reaction were dried and all reactions for preparing monomers were carried out under Nitrogen atmosphere and the reaction for preparing polymer was carried under Argon atmosphere.

### Measurements

Polymer solutions in **tetrahydrofuran** (THF) at 100 °C were used as samples for Gel permeation chromatography (GPC) analysis. The GPC curves were recorded on the equipment consisting of Waters Model 515 HPLC Pump, GILSON Model 234 Autoinjector, MILLIPORE Waters Lambda-Max Model 481 LC Spectrometer, Erma ERC-7512 RI Detector, PLgel 5m 500A Column, and PLgel 10m MIXED-B Column using THF as the eluent at a rate of 1 cm<sup>3</sup> minute<sup>-1</sup>. The GPC curves were obtained by the RI-detection method, which was calibrated with a series of polystyrene narrow standards (Polymer Laboratories). Nuclear magnetic resonance (NMR) Spectra were recorded on Bruker DRX-500 MHz NMR spectrometers and has variable temperature capabilities of ca. ± 100 °C in 1,1,2,2-tetrachloroethane-d<sub>2</sub> solution. FTIR absorption spectra were recorded on the Nicolet Model 205 FT-IR Spectrometer using a Diamond ATR attachment for solid samples analysis. Elemental analysis was carried out by the Perkin Elmer 2400 CHN Elemental Analyser for CHN analysis and by the Schöniger oxygen flask combustion method for anion analysis. The weights of the samples submitted for analysis were approx. 5 mg for CHN analysis and approx. 5 mg for each anion analysis. UV-visible absorption spectra were measured by Hitachi U-2010 Double Beam UV / Visible Spectrophotometer. The absorbance of polymers was measured in solution of toluene (spectrophotometric grade) and THF (spectrophotometric grade) at ambient temperature using rectangular quartz cuvettes (light path length = 10 mm) purchased from Sigma-Aldrich. Samples of pristine polymer thin films for UV-visible absorption spectra measurements were prepared by dip coating quartz plates into 1 mg cm<sup>-3</sup> polymer solutions in chloroform (HPLC grade) and the measurements were carried out at ambient temperature. Cyclic voltammograms (CV) were recorded using a Princeton Applied Research Model 263A Potentiostat/Galvanostat. Measurements were carried out under an inert argon atmosphere at 25 ± 2 °C. Tetrabutylammonium perchlorate (TBAClO<sub>4</sub>) 10 cm<sup>3</sup> solution in acetonitrile (HPLC) (0.1 mol dm<sup>-3</sup>) was used as the electrolyte solution. A three electrode system was used consisting of an Ag/Ag<sup>+</sup> reference electrode (silver wire in 0.01 mol dm<sup>-3</sup> silver nitrate solution in the electrolyte solution), a platinum working electrode (2 mm-diameter smooth platinum disc, area = 3.14 × 10<sup>-2</sup> cm<sup>2</sup>), and a platinum counter electrode (platinum wire). Polymer thin films were formed by drop casting 1.0 mm<sup>3</sup> of polymer solutions in dichloromethane (HPLC grade) (1 mg cm<sup>-3</sup>) onto the working electrode, then dried in air. Ferrocene was employed as a reference redox system according to IUPAC's recommendation. Polymer thin films were formed by drop-casting 1.0 mm<sup>3</sup> of polymer solutions in dichloromethane (DCM) (analytical reagent, 1 mg cm<sup>-3</sup>) onto the working electrode and dried in the air.

### The thienothiophene-based Copolymer: P1, P2 and P3

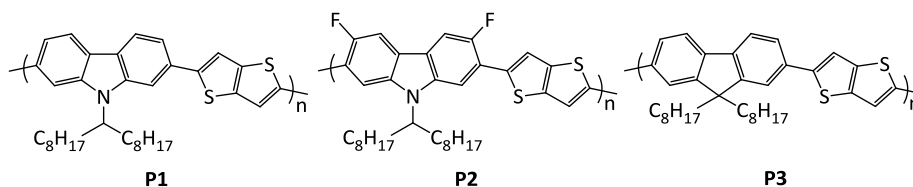


Figure 1. Structure of copolymers **P1**, **P2** and **P3**.

Figure 1 shows a series of copolymer, two of them are carbazole based on polycarbazole poly(9-(heptadecan-9-yl)-9H-carbazole-*alt*-thieno[3,2-*b*]thiophene) (**P1**) and poly(3,6-difluoro-9-(heptadecan-9-yl)-9H-carbazole-*alt*-thieno[3,2-*b*]thiophene) (**P2**), and one is fullerene based poly(9,9-dioctyl-9H-fluorene-*alt*-thieno[3,2-*b*]thiophene) (**P3**). All of them contain the same thienothiophene-based repeat units. All synthesis of copolymers were performed using a modified Suzuki Cross Coupling procedure by Iraqi et al. [28]. These polymers were chosen due to similarities in their composition with polymers made previously by the Iraqi group, and also in the literatures [12,

29-31]. To improve the internal charge transfer and achieve low bandgap conjugated polymers, the heterocyclic thienothiophene has been utilized in preparing donor-acceptor system, which is more complex molecular structure and consist of more atoms in the alternating donor and acceptor units [28, 32].

#### General Method for the Polymerization P1, P2 and P3

A 100 ml one necked flask under argon containing *monomer A* (0.379 mmol) and *monomer B* (0.379 mmol) in dry toluene (8 ml) was degassed. To the mixture 20 % tetraethylammonium hydroxide (2.8 ml, previously degassed 2.5 h) was added and degassed. Then Pd(OAc)<sub>2</sub> (11.23 mg, 0.05 mmol) and tri(o-toly)phosphine (38.05 mg, 0.13 mmol) were added, the system was degassed under argon and heated to 90 °C. There was precipitate out of solution after 1 h and the mixture was cooled to room temperature and then bromobenzene (0.10 ml, 0.15 g, 0.94 mmol) was added, degassed and heated to 90 °C for 1 h. Then, the mixture was cooled to room temperature and phenylboronic acid (0.12 g, 0.98 mmol) was added, degassed and heated to 90 °C for 3 h. After cooling to room temperature, CHCl<sub>3</sub> (200 ml) was added to solubilise the polymer. An ammonium hydroxide solution (28 % in H<sub>2</sub>O, 50 ml) was then added and the mixture was stirred overnight. Then the organic phase was separated and washed with distilled water (2 x 250 ml), concentrated to approximately 50 ml and poured into degassed methanol/water (10:1, v:v, 300 ml). The resulting mixture was then stirred overnight and filtered through a membrane filter. The collected solid was cleaned using a Soxhlet extraction with solvents in order methanol (250 ml), acetone (250 ml), hexane (250 ml), and toluene (250 ml). The toluene fractions were concentrated to approximately 50 ml and then poured into degassed methanol (500 ml), the resulting mixtures stirred overnight and the solid was collected by filtration through a membrane filter. All the fractions of **yield** were dark red powder.

#### Poly(9-(heptadecan-9-yl)-9H-carbazole-alt-thieno[3,2-b]thiophene) (P1)

*Monomer A* (9-(Heptadecan-9-yl)-2,7-bis(4,4,5,5-tetramethyl-1,3,2-dioxaborolan-2-yl)-9H-carbazole) and *Monomer B* (2,5-dibromothieno[3,2-b]thiophene) All the fractions of **P1** were dark red powder. Toluene fraction, yield: 65.7 mg (32 %). GPC (1, 2, 4-trichlororbenzene at 100 °C): M<sub>w</sub> = 6500, M<sub>n</sub> = 2800, PD = 2.3. <sup>1</sup>H NMR (C<sub>2</sub>D<sub>2</sub>Cl<sub>4</sub>), (δ<sub>H</sub>/ppm): 8.18 (d, 2H); 7.84 (d, 2H); 7.80-7.65 (bm, 2H); 7.60-7.45 (bm, 2H); 4.62 (br, 1H); 2.33 (br, 4H); 2.10-1.98 (br, 4H); 1.41 (d, 4H); 1.38-1.01 (bm, 16H); 0.93-0.71 (bm, 6H). FT-IR (cm<sup>-1</sup>): 3079, 2960, 2923, 2853, 2159, 1981, 1621, 1598, 1561, 1509. Elemental analysis (%) calculated for C<sub>35</sub>H<sub>43</sub>NS<sub>2</sub>: C, 77.58; H, 8.00; N, 2.58; Br, 0 Found: C, 77.06; H, 8.01; N, 2.22; Br, 0.

#### Poly(3,6-difluoro-9-(heptadecan-9-yl)-9H-carbazole-alt-thieno[3,2-b]thiophene) (P2)

*Monomer A* (3,6-difluoro-9-(heptadecan-9-yl)-2,7-bis(4,4,5,5-tetramethyl-1,3,2-dioxaborolan-2-yl)-9H-carbazole) and *Monomer B* (2,5-dibromothieno[3,2-b]thiophene). All the fractions **P2** were dark red powder. Toluene fraction, yield: 131 mg (60 %). GPC (1, 2, 4-trichlororbenzene at 100 °C): M<sub>w</sub> = 7 100, M<sub>n</sub> = 2 800, PD = 2.4. <sup>1</sup>H NMR (C<sub>2</sub>D<sub>2</sub>Cl<sub>4</sub>), (δ<sub>H</sub>/ppm): 8.15 (d, 2H); 7.80 (d,2H); 7.78-7.60 (bm, 2H); 4.77 (br, 1H), 2.50-2.28 (br, 4H); 2.09-1.92 (br, 4H); 1.42 (bm, 4H); 1.38-0.98 (bm, 16H); 0.84 (br, 6H). FT-IR (cm<sup>-1</sup>): 2922, 2852, 2184, 1611, 1569, 1527, 1452. Elemental analysis (%) calculated for C<sub>35</sub>H<sub>41</sub>F<sub>2</sub>NS<sub>2</sub>: C, 72.75; H, 7.15; N, 2.42; Br, 0. Found: C, 72.00; H, 7.55; N, 2.00; Br, 0.

#### Poly(9,9-dioctyl-9H-fluorene-alt-thieno[3,2-b]thiophene) (P3)

*Monomer A* (9,9-dioctylfluorene-2,7-diboronic acid bis(1,3-propanediol) ester) and *monomer B* (2,5-dibromothieno[3,2-b]thiophene). All the fractions **P3** were dark red powder. Toluene fraction, yield: 107 mg (54 %). GPC (1, 2, 4-trichlororbenzene at 100 °C): M<sub>w</sub> = 4600, M<sub>n</sub> = 2100, PD = 2.2. <sup>1</sup>H NMR (C<sub>2</sub>D<sub>2</sub>Cl<sub>4</sub>), (δ<sub>H</sub>/ppm): 8.45 (d, 2H); 8.18-8.03 (d, 2H); 7.81-7.68 (bm, 4H); 1.18 (br, 4H); 1.59 (br, 4H); 1.43-1.20 (bm, 20H); 0.82 (br, 6H). FT-IR (cm<sup>-1</sup>): 3043, 2956, 2923, 2852, 1975, 1623, 1528, 1489, 1462. Elemental analysis (%) calculated for C<sub>35</sub>H<sub>42</sub>S<sub>2</sub>: C, 79.79; H, 8.04; Br, 0. Found: C, 79.02; H, 8.55; Br, 0.

## Results and Discussion

### Synthesis and Characterization

All these copolymers were synthesized using Suzuki Cross Coupling reactions, in the presence of Pd(OAc)<sub>2</sub> and tri(o-tolyl)phosphine (1:2) as catalysts [32, 33]. The first step involves an oxidative addition of palladium (0) to the aryl bromide to form a palladium (II). The second step involves reaction with the base to produce an intermediate complex, which in the third step forms the organopalladium via transmetalation with the boronic ester in the second

monomer. Finally, the polymer is obtained by reductive elimination, which restores the original palladium (0) and then the catalytic cycle starts again [34]. The polymerization of **P1-P3** was performed twice in different conditions, the first one was carried out in THF as solvent and NaHCO<sub>3</sub> as base, in the second polymerization, toluene was used as solvent and tetraethylammonium hydroxide as base, due to the high boiling point of toluene, the average molecular weights of the polymers obtained from this polymerization was higher than those from the first polymerization. All polymerizations were performed under argon in degassed systems, and they were stopped when the solutions became too viscous.

<sup>1</sup>H-NMR studies conducted at 100 °C in 1,1,2,2-tetrachloroethane-d<sub>2</sub> (C<sub>2</sub>D<sub>2</sub>Cl<sub>4</sub>) on **P1** confirmed its assigned structure. The <sup>1</sup>H-NMR spectrum of **P1** is reveals in the aromatic region the protons of the carbazole hydrogen with multiplet signal at 8.10 ppm, 7.78 ppm and 7.53 ppm assigned to protons a, b and c respectively. The two protons on the thienothiophene repeat units are observed at broad peak 7.53 ppm. The broad peak at 4.61 ppm corresponds to the proton on the carbon atom at position e. Other peaks correspond to alkyl chains which are connected to carbazole units. <sup>1</sup>H-NMR studies conducted at 100 °C in 1,1,2,2-tetrachloroethane-d<sub>2</sub> on **P2** confirmed its assigned structure. The <sup>1</sup>H-NMR spectrum of **P2** is reveals in the aromatic region proton on the carbazole units with multiplet signal at 8.18 ppm and 7.78 ppm assigned to protons a and b respectively. The two protons on the thienothiophene repeat units are observed at broad peak 7.78 ppm and overlap with the carbazole proton at position b. The broad peak at 4.77 ppm corresponds to the proton on the carbon atom at position d. Other peaks correspond to alkyl chains which are connected to carbazole units. <sup>1</sup>H-NMR studies conducted at 100 °C in 1,1,2,2-tetrachloroethane-d<sub>2</sub> on **P3** confirmed its assigned structure. The <sup>1</sup>H-NMR spectrum of **P3** is reveals in the aromatic region the proton of the fluorene hydrogen with multiplet signal at 8.51 ppm, 8.19 ppm and 7.83 ppm assigned to protons a, b and c respectively. The two protons on the thienothiophene repeat units are observed at broad peak 7.83 ppm and overlap with the fluorene proton at position c. Other peaks correspond to alkyl chains which are connected to fluorene units. The IR spectrum of **P1** was fairly similar patterns to those of its constituent monomers with some assignments of different bands/peaks. It can be seen the characterizing peak at 3083 cm<sup>-1</sup> which falls in relation to aromatic benzene groups =C–H stretch. The characteristic peaks at 2961 cm<sup>-1</sup> and 2853 cm<sup>-1</sup> are assigned to the alkyl stretching frequencies of the methylene groups.

The characteristic overtones are seen from about 2000-1665 cm<sup>-1</sup>. The assignment of different peaks compare to monomer 9-(heptadecan-9-yl)-2,7-bis(4,4,5,5-tetramethyl-1,3,2-dioxaborolan-2-yl)-9*h*-carbazole was observed at 1463 cm<sup>-1</sup>, 1410 cm<sup>-1</sup> and 1260 cm<sup>-1</sup> and it has a mixture of peaks related to the combination bands and also the deformations bands of the aromatic -CH groups and methylene -CH<sub>2</sub>- groups. The peak originally at 1037cm<sup>-1</sup>, attributed to C<sub>aromatic</sub>-Br linkage in the spectrum of monomer 2,5-dibromothieno[3,2-*b*]thiophene disappeared. And also peaks at 1327 cm<sup>-1</sup> and 1296 cm<sup>-1</sup> (B-O stretch), and 1140 cm<sup>-1</sup> (B-C stretch) presents in the spectrum of (**7**) did also disappear from the spectrum of **P1** due to the consumption of the corresponding functional groups in the Suzuki cross-coupling reaction. The IR spectrum of the **P2** was fairly similar patterns to those of its constituent monomers with some assignments of different bands/peaks. It can be seen the characterizing peak at 3094 cm<sup>-1</sup> which falls in relation to aromatic benzene groups =C–H stretch. The characteristic peaks at 2960 cm<sup>-1</sup>, 2923 cm<sup>-1</sup> and 2852 cm<sup>-1</sup> are assigned to the alkyl stretching frequencies of the methylene groups. The characteristic overtones are seen from about 2161-1665 cm<sup>-1</sup>. The assignment of different peaks compare to monomer 3,6-difluoro-9-(heptadecan-9-yl)-2,7-bis(4,4,5,5-tetramethyl-1,3,2-dioxaborolan-2-yl)-9*H*-carbazole was observed at 1455 cm<sup>-1</sup>, 1431 cm<sup>-1</sup> and 1335 cm<sup>-1</sup> and its has a mixture of peaks related to the combination bands and also the deformations bands of the aromatic -CH groups and methylene -CH<sub>2</sub>- groups. Peaks at 1258 cm<sup>-1</sup> are characteristic to the C-N bond and a peak at 1079 cm<sup>-1</sup> and 1017 cm<sup>-1</sup> is assigned to the C-F bonds. The peak originally at 1037cm<sup>-1</sup>, attributed to C<sub>aromatic</sub>-Br linkage in the spectrum of monomer 2,5-dibromothieno[3,2-*b*]thiophene disappeared. And also peaks at 1327 cm<sup>-1</sup> and 1296 cm<sup>-1</sup> (B-O stretch), and 1140 cm<sup>-1</sup> (B-C stretch) present in the spectrum of 3,6-difluoro-9-(heptadecan-9-yl)-2,7-bis(4,4,5,5-tetramethyl-1,3,2-dioxaborolan-2-yl)-9*H*-carbazole did also disappear from the spectrum of **P2** due to the consumption of the corresponding functional groups in the Suzuki cross-coupling reaction.

The IR spectrum of the **P3** has fairly similar patterns to those of its constituent monomers with some assignments of different bands/peaks. The character peak in relation to aromatic benzene groups =C–H stretch can seen at 3085 cm<sup>-1</sup>. The characteristic peaks at 2959 cm<sup>-1</sup>, 2920 cm<sup>-1</sup> and 2850 cm<sup>-1</sup> are assigned to the alkyl stretching frequencies

of the methylene groups. The characteristic overtones are seen from about 2170-1721  $\text{cm}^{-1}$ . The assignment of different peaks compare to monomer 9,9-dioctylfluorene-2,7-diboronic acid bis(1,3-propanediol) ester was observed at 1499  $\text{cm}^{-1}$ , 1453  $\text{cm}^{-1}$  and 1335  $\text{cm}^{-1}$  and its has a mixture of peaks related to the combination bands and also the deformations bands of the aromatic  $-\text{CH}$  groups and methylene  $-\text{CH}_2-$  groups.

The peak originally at 1037 $\text{cm}^{-1}$ , attributed to  $\text{C}_{\text{aromatic}}-\text{Br}$  linkage in the spectrum of monomer 2,5-dibromothieno[3,2-*b*]thiophene disappeared. And also peaks at 1327  $\text{cm}^{-1}$  and 1296  $\text{cm}^{-1}$  (B-O stretch), and 1140  $\text{cm}^{-1}$  (B-C stretch) present in the spectrum of 9,9-dioctylfluorene-2,7-diboronic acid bis(1,3-propanediol) ester did also disappear from the spectrum of **P3** due to the consumption of the corresponding functional groups in the Suzuki cross-coupling reaction.

The yields quoted for the polymers in Table 1 are the yields after Soxhlet extraction of the polymers. Analysis of the polymers was conducted on the highest molecular weight fractions which will be used in the actual photovoltaic devices. Gel permeation chromatography measurements were taken in 1, 2, 4-trichlororbenzene (TCB) at 100 °C as at lower temperatures it was not possible to solubilise all the higher molecular weight polymer fractions to obtain the true molecular weights. GPC results from the polymerization for polymers **P1**, **P2** and **P3** by using polystyrene standards are shown in Table 1.

Table 1. GPC data of **P1**, **P2** and **P3**

Polymer	Yield (%)	$M_w$	$M_n$	PDI
<b>P1</b>	32	6500	2800	2.3
<b>P2</b>	60	7100	2900	2.4
<b>P3</b>	54	4600	2100	2.2

Polymer **P1** was obtained as a red solid in 32 % yield. GPC analysis of chloroform fraction of polymer **P1** gave an  $M_w = 6500$  and  $M_n = 2800$  with a polydispersity of 2.3. Polymer **P2** was obtained as a red solid in 60 % yield. GPC analysis of chloroform fraction of polymer **P2** gave an  $M_w = 7100$  and  $M_n = 2900$  with a polydispersity of 2.4. Polymer **P3** was also obtained as a red solid in 54 % yield. GPC analysis of chloroform fraction of polymer **P3** gave an  $M_w = 4600$  and  $M_n = 2100$  with a polydispersity of 2.2. Based on the Table 1, polydispersity of **P3** is lower than polymers **P1** and **P2**. It is due to the rich alternating electron along their backbone which is presence from carbazole and fluorine linked compare with the limited alternating electron in fluorine in **P3** as the compound backbone.

Elemental analysis was used to check if a sample is consistent with a given molecular formula by using qualitative analysis technique. Clearly shows no bromine content, indicating that the terminal groups were end-capped in polymers **P1**, **P2** and **P3**. The elemental analysis of the other elements of polymers **P1**, **P2** and **P3** did also give a satisfactory agreement with their proposed structure.

### Optical and Electrochemical Properties

The UV-Visible absorption spectra of the polymers were measured in chloroform and in solid state as thin films. The optical band gaps were calculated from the onset of absorption of the polymers in the solid state, the results of these studies are summarized in Table 2.

Table 2. UV-Vis data of **P1**, **P2** and **P3**

Polymers	$\lambda_{\text{max}}$ Solution (nm)	$\lambda_{\text{max}}$ Thin film (nm)	$\lambda_{\text{Onset}}$ Abs. (nm)	$E_g$ Optical (eV)
<b>P1</b>	435	442	505	2.46
<b>P2</b>	405	419	525	2.36
<b>P3</b>	395	400	503	2.47

Figure 2 shows the absorption spectra of **P1** in solution (chloroform) and in the solid state. Polymer **P1** displays a maximum absorption in solution at  $\lambda_{\text{max}} = 435$  nm. The electronic spectra of polymer **P1** in the solid state display similar features to those in solution with a  $\lambda_{\text{max}} = 442$  nm with a shoulder peak at 505 nm, indicating more extended electronic conjugation in films than in solution. The optical band gap of polymer **P1** as determined from the onset of its absorption spectra in the solid state and has a value  $E_g = 2.46$  eV.

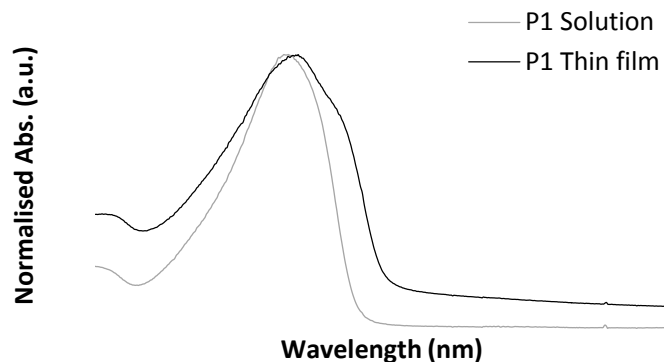


Figure 2. Normalised UV-Vis spectra of **P1** in chloroform solution (grey line) and a thin film (black line).

Figure 3 shows the absorption spectra of **P2** in solution (chloroform) and in the solid state. Polymer **P2** displays a maximum absorption in solution at  $\lambda_{\text{max}} = 405$  nm with a shoulder absorption band at 511 nm. The shoulder absorption peak can be explained by the existence of segments of more extended electronic conjugation along the polymer chains. The electronic spectra of polymer **P2** in the solid state display similar features to those in solution with a  $\lambda_{\text{max}} = 419$  nm and a shoulder peak at 525 nm, indicating more extended electronic delocalization in **P2** as on films. The optical band gap of polymer **P2** as determined from the onset of its absorption spectra in the solid state has a value  $E_g = 2.36$  eV. The presence of fluorine substitutes at the 3,6-position of carbazole repeat units on **P2** has led into a monomer band gap in the polymer when it is composed to that of the equivalent polymer without fluorine substituent **P1**. This indicates the present of fluorine interactions of **P2** with neighboring sulfur or hydrogen atoms of the thienothiophene repeat units along the polymer backbone.

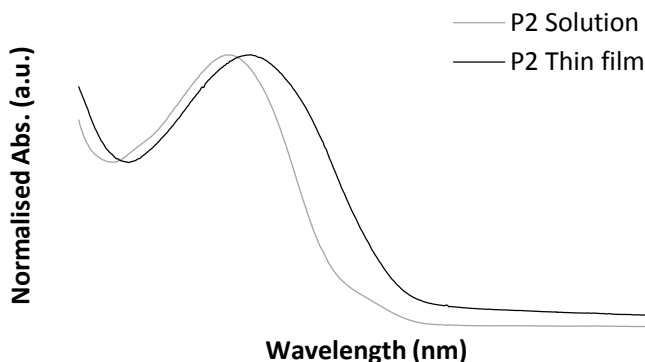


Figure 3. Normalised UV-Vis spectra of **P2** in chloroform (grey line) and a thin film (black line).

Figure 4 shows the absorption spectra of **P3** in solution (chloroform) and in the solid state. Polymer **P3** displays a maximum absorption in solution at  $\lambda_{\text{max}} = 395$  nm. The electronic spectra of polymer **P3** in the solid state display similar features to those in solution with a  $\lambda_{\text{max}} = 400$  nm. The optical band gap of polymer **P3** as determined from the onset of its absorption spectra in the solid state has a value  $E_g = 2.47$  eV. This indicates similar electronic properties between the polymers with little differences in their electronic delocalization or simple change of carbazole to fluorene repeat units.

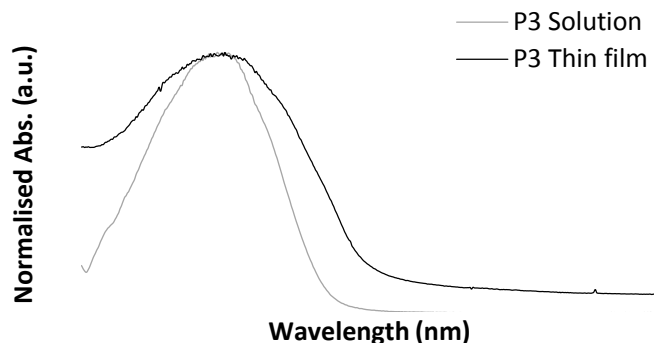


Figure 4. Normalised UV-Vis spectra of **P3** in chloroform (grey line) and a thin film (black line).

Investigations of the electrochemical properties of polymers **P1**, **P2** and **P3** were also undertaken in cyclic voltammetry (CV) performed on drop-cast polymer films in acetonitrile with tetrabutylammonium perchlorate as the electrolyte. The LUMO level and the HOMO level were calculated from the onset reduction and oxidation respectively. Then, the electrochemical band gap ( $E_g$ ) can be calculated from the difference between them. The cyclic voltammogram of the polymers **P1**, **P2** and **P3** are shown in Figure 5.

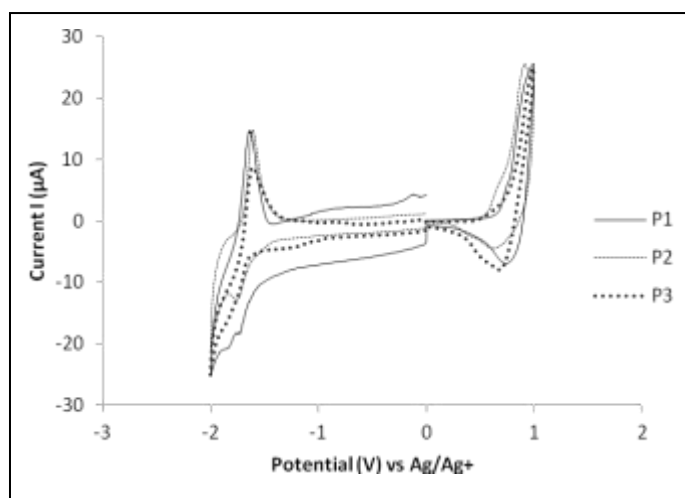


Figure 5. Normalised cyclic voltammogram of **P1**, **P2** and **P3**.

All values were taken relative to the reference electrode Ag/Ag<sup>+</sup>, on the basis that the energy level of the ferrocene/ferrocenium is 4.8 eV below the vacuum level and oxidation occurs at 0.082 V data from the spectra were adjusted

to give the polymers relative to these values [35]. Polymer **P1** exhibits an oxidation wave at  $E_{pa} = 0.98$  V and a reduction wave at  $E_{pa} = -1.65$  V, and their associated reduction and oxidation waves at  $E_{pc} = 0.74$  V and  $E_{pc} = -1.76$  V, respectively. From the onset of oxidation (0.65 V) and the onset of reduction (-1.53 V), the HOMO level is at -5.45 eV and the LUMO level is at -3.27 eV for the polymer backbone (on the basis that ferrocene/ferrocenium has an IP of 4.8 eV below the vacuum level and the oxidation occurs at 0.082 V relative to  $Ag/Ag^+$ ), therefore the electrochemical band gap of the polymer is 2.18 eV. Polymer **P2** exhibits an oxidation wave at  $E_{pa} = 1.10$  V and a reduction wave at  $E_{pa} = -1.65$  V, and their associated reduction and oxidation waves at  $E_{pc} = 0.75$  V and  $E_{pc} = -1.74$  V, respectively. From the onset of oxidation (0.70 V) and the onset of reduction (-1.63 V), the HOMO level is at -5.50 eV and the LUMO level is at -3.17 eV for the polymer backbone (on the basis that ferrocene/ferrocenium has an IP of 4.8 eV below the vacuum level and the oxidation occurs at 0.082 V relative to  $Ag/Ag^+$ ), therefore the electrochemical band gap of the polymer is 2.33 eV. Polymer **P3** exhibits an oxidation wave at  $E_{pa} = 1.17$  V and a reduction wave at  $E_{pa} = -1.62$  V, and their associated reduction and oxidation waves at  $E_{pc} = 0.82$  V and  $E_{pc} = -1.77$  V, respectively. From the onset of oxidation (0.84 V) and the onset of reduction (-1.60 V), the HOMO level is at -5.64 eV and the LUMO level is at -3.20 eV for the polymer backbone (on the basis that ferrocene/ferrocenium has an IP of 4.8 eV below the vacuum level and the oxidation occurs at 0.082 V relative to  $Ag/Ag^+$ ), therefore the electrochemical band gap of the polymer is 2.44 eV as shown in Table 3.

Table 3. Voltammetry results and band gaps of **P1**, **P2** and **P3**

Polymers	$E_{onset, ox}$	$E_{onset, red}$	HOMO (eV)	LUMO (eV)	Band gap (eV)
	(V) <sup>a)</sup>	(V) <sup>a)</sup>			
<b>P1</b>	0.65	-1.53	-5.45	-3.27	2.18
<b>P2</b>	0.70	-1.63	-5.50	-3.17	2.33
<b>P3</b>	0.84	-1.60	-5.64	-3.20	2.44

<sup>a)</sup> vs.  $Ag/Ag^+$

The band gap **P3** is higher compare to **P1** and **P2**. It is due to associated reduction and oxidation waves the polymer **P1** and **P2** with fluorine substituents has or more extended electronic delocalisation. These results also point to the presence of interactions between the fluorine substituents on carbazole repeat units on **P2**.

#### Thermogravimetric Analysis (TGA)

The thermal stability of **P1**, **P2** and **P3** were investigated in this study. The thermogram of **P1**, **P2** and **P3** is shown in Figure 6 and the details of the TGA results are shown in Table 4.

Figure 6 shows the TGA curves for of the thermal degradation of the polymer **P1**, the onset of the degradation occurs at 318 °C, the onset of second degradation is 430 °C with a weight loss of 73.1 %. The percentage of residual weight 26.9 % is consistent with percentage weight of the polymer backbone. The TGA analysis confirms that the polymer has high thermal stability up to 380 °C. Thermal gravimetry analysis measurements revealed the remarkable stability of the polymer up to 430 °C, which indicated that these polymers are thermally very stable. The subsequent degradation and weight loss of the polymer beyond 430 °C was proportional to the mass of it's an alkyl-group substituents. The polymer did not show any further weight loss up to a temperature of 800 °C. Figure 6 shows the TGA curves for of the thermal degradation of the polymer **P2**, the onset of the degradation occurs at 311 °C, the onset of second degradation is 432 °C with a weight loss of 72.9 %. The percentage of residual weight 27.1 % is consistent with percentage weight of PDI units and polymer backbone. The TGA analysis confirms that the polymer has high thermal stability up to 380 °C. Thermal gravimetry analysis measurements revealed the remarkable stability of the polymer up to 432 °C, which indicated that these polymers are thermally very stable. The subsequent degradation and weight loss of the polymer beyond 432 °C was proportional to the mass of its alkyl-group substituents. The polymer did not show any further weight loss up to a temperature of 800 °C. Based on the

thermogram as shows in the Figure 6 TGA curves of the thermal degradation of the polymer **P3**, the onset of the degradation occurs at 291 °C, the onset of second degradation is 425 °C with a weight loss of 72 %. The percentage of residual weight 28 % is consistent with percentage weight of PDI units and polymer backbone. The TGA analysis confirms that the polymer has high thermal stability up to 380 °C. Thermal gravimetry analysis measurements revealed the remarkable stability of the polymer up to 425 °C, which indicated that these polymers are thermally very stable. The subsequent degradation and weight loss of the polymer beyond 425 °C was proportional to the mass of it an alkyl-group substituents. The polymer did not show any further weight loss up to a temperature of 800 °C.

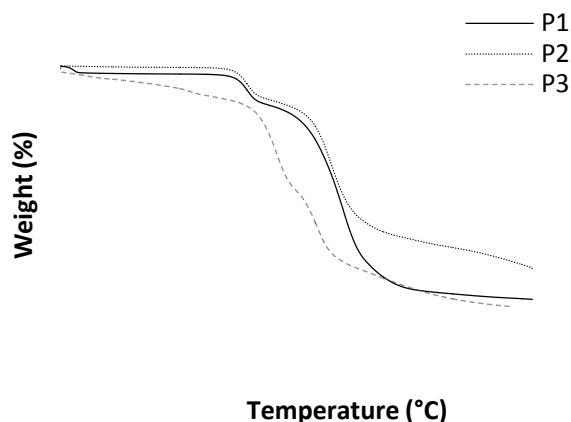


Figure 6. The TGA thermogram of **P1**, **P2** and **P3**.

Table 4. The TGA and DSC data of **P1**, **P2** and **P3**

Polymers	TGA Analysis		Weight loss at 800 °C (wt. %)	DSC Analysis $T_g / ^\circ\text{C}$
	Onset degradation temp. / °C 1 <sup>st</sup> degradation	2 <sup>nd</sup> degradation		
<b>P1</b>	318	430	73.1	70
<b>P2</b>	311	432	72.9	78
<b>P3</b>	291	425	72.0	76

#### Differential Scanning Calorimetry (DSC) Analysis

Table 4 summarises the results from the thermo gravimetric analysis (TGA) and the differential scanning calorimetry (DSC). In applications that can experience temperature extremes, it is important to know what will happen when these polymers are exposed to variants in temperature and how they will affect the mechanical behaviour of the polymer. The glass transition ( $T_g$ ) is obtained from the DSC trace and it is a function of polymer backbone flexibility. The polymers were subjected to a first heating run, cooling run followed by further heating run, at the scan rate 10 °C/ min, and when no  $T_g$  was seen, 20 up to 100 °C/ min rates was applied. The glass transitions ( $T_g$ ) value were estimated and obtained from the first scans as broad peaks, they were above 50 °C indicating that all polymers have good tolerance to the stages required in making devices. Based on the table the  $T_g$  of **P1**, **P2** and **P3** were 70 °C, 78 °C and 76 °C, respectively. All the  $T_g$  results of the polymers are similar to each other, due to the present of thienothiophene, which provide more flexibility for the polymer backbones.

### Conclusion

All polymers **P1-P3** were successfully obtained in yields ranging from 32 % to 60 %. UV-Vis analysis showed the polymer absorbed at high wavelengths  $\lambda_{\max}$  435 nm in solution and 442 nm in the solid state and the band gap of **P1** in solid state is 2.46 eV. CV measurements estimated the band gap as 2.18 eV from the onset of oxidation and reduction. The HOMO and LUMO levels can be estimated as -5.45 eV and -3.27 eV respectively. These results are in agreement with the design procedures for the use of these materials in photovoltaic applications. The optical band gap,  $E_g$  of polymers **P1**, **P2** and **P3** were 2.46 eV, 2.36 eV and 2.47 eV respectively. The photophysical properties of these polymers show that **P2** has the narrowest optical band gap due to the electrostatic interaction between the hydrogens at the 4-position on thienothiophene rings and the fluorine substituents on the neighbouring carbazole repeat units. All polymers **P1 - P3** have fairly low molecular weights as a result of their low solubility and their precipitation out of solution during the polymerisation reaction. The presence of fluorine substituents at the 3,6-position of carbazole repeat units on **P2** has led into a monomer band gap in the polymer when it is composed to that of the equivalent polymer without fluorine substituent **P1**. This indicates the presence of fluorine interactions of **P2** with neighboring sulfur or hydrogen atoms of the thienothiophene repeat units along the polymer backbone.

### Acknowledgement

We would like to acknowledge the financial support of the University of Malaysia Sabah and Ministry of Education Malaysia for their financial support over the period of this research.

### References

1. Yao, Y., Dong, H., and Hu, W. (2013) Ordering of conjugated polymer molecules: recent advances and perspectives. *Polymer Chemistry*, 4: 5197-5205.
2. Jenekhe, S. A. and Zhu, D. (2013) Conjugated polymers. *Polymer Chemistry*, 4, 5142-5143.
3. Chen, Y.-C., Yu, C.-Y., Fan, Y.-L., Hung, L.-I., Chen, C.-P., and Ting, C. (2010) Low-bandgap conjugated polymer for high efficient photovoltaic applications. *Chemical Communications*, 46, 6503-6505.
4. Prim, D. and Kirsch, G. (1994) Synthesis of new 2-arylthieno [3, 2-b] thiophenes. *Journal of Chemical Society Perkin Transactions 1*: 2603-2606.
5. Masresha, T. (2006) Photovoltaic properties of polymer based bulk heterojunction solar cell composed of poly[3-(2,5-dioctyle-phenyl) thiophene](PDOPT) and (PCBM). *MSc Thesis*. Addis Ababa University.
6. Raj, M. R. and Anandan, S. (2013) Donor conjugated polymers-based on alkyl chain substituted oligobenzoc[3,2-b]thiophene derivatives with well-balanced energy levels for bulk heterojunction solar cells. *RSC Advances*, 3: 14595-14608.
7. Voortman, T. P., De Gier, H. D., Havenith, R. W. A., and Chiechi, R. C. (2014) Stabilizing cations in the backbones of conjugated polymers. *Journal of Materials Chemistry C*, 2: 3407-3415.
8. Printz, A. D., Savagatrup, S., Burke, D. J., Purdy, T. N., and Lipomi, D. J. (2014) Increased elasticity of a low-bandgap conjugated copolymer by random segmentation for mechanically robust solar cells. *RSC Advances*, 4: 13635-13643.
9. Hoppe, H. and Sariciftci, N. S. (2006). Morphology of polymer/fullerene bulk heterojunction solar cells. *Journal of Materials Chemistry*, 16: 45-61.
10. Biniek, L., Chochos, C. L., Leclerc, N., Hadziioannou, G., Kallitsis, J. K., Bechara, R., Leveque, P., and Heiser, T. (2009). A [3,2-b]thienothiophene-alt-benzothiadiazole copolymer for photovoltaic applications: design, synthesis, material characterization and device performances. *Journal of Materials Chemistry*, 19: 4946-4951.
11. Choy, N., Russell, K. C., Alvarez, J. C., and Fider, A. (2000). Synthesis and redox properties of novel alkynyl flavins. *Tetrahedron Letters*, 41: 1515-1518.
12. Mohamad, D. K., Fischereder, A., Yi, H., Cadby, A. J., Lidzey, D. G., and Iraqi, A. (2011). A novel 2,7-linked carbazole based "double cable" polymer with pendant perylene diimide functional groups: preparation, spectroscopy and photovoltaic properties. *Journal of Materials Chemistry*, 21: 851-862.
13. Peet, J., Wen, L., Byrne, P., Rodman, S., Forberich, K., Shao, Y., Drolet, N., Gaudiana, R., Dennler, G., and Waller, D. (2011). Bulk heterojunction solar cells with thick active layers and high fill factors enabled by a bithiophene-co-thiazolothiazole push-pull copolymer. *Applied Physics Letters*, 98: 043301.

14. Bronstein, H., Chen, Z., Ashraf, R. S., Zhang, W., Du, J., Durrant, J. R., Shakya Tuladhar, P., Song, K., Watkins, S. E., Geerts, Y., Wienk, M. M., Janssen, R. a. J., Anthopoulos, T., Sirringhaus, H., Heeney, M., and McCulloch, I. (2011). Thieno[3,2-b]thiophene–Diketopyrrolopyrrole-Containing Polymers for High-Performance Organic Field-Effect Transistors and Organic Photovoltaic Devices. *Journal of the American Chemical Society*, 133: 3272-3275.
15. Baek, M.-J., Lee, S.-H., Zong, K., and Lee, Y.-S. (2010). Low band gap conjugated polymers consisting of alternating dodecyl thieno[3,4-b]thiophene-2-carboxylate and one or two thiophene rings: Synthesis and photovoltaic property. *Synthetic Metals*, 160: 1197-1203.
16. Chang, S.-W., Waters, H., Kettle, J., Kuo, Z.-R., Li, C.-H., Yu, C.-Y., and Horie, M. (2012) Pd-Catalysed Direct Arylation Polymerisation for Synthesis of Low-Bandgap Conjugated Polymers and Photovoltaic Performance. *Macromolecular Rapid Communications*, 33 (22):1927-1932.
17. Duan, C., Huang, F., and Cao, Y. (2012) Recent development of push-pull conjugated polymers for bulk-heterojunction photovoltaics: rational design and fine tailoring of molecular structures. *Journal of Materials Chemistry*, 22: 10416-10434.
18. He, X. and Baumgartner, T. (2013). Conjugated main-group polymers for optoelectronics. *RSC Advances*, 3: 11334-11350.
19. Yang, L., Tumbleston, J. R., Zhou, H., Ade, H., and You, W. (2013) Disentangling the impact of side chains and fluorine substituents of conjugated donor polymers on the performance of photovoltaic blends. *Energy & Environmental Science*, 6: 316-326.
20. Sharma, G. D., Singh, M., Kurchania, R., Koukaras, E. N., and Mikroyannidis, J. A. (2013). Synthesis and characterization of two carbazole-based alternating copolymers with 4-nitrophenylcyanovinylene pendant groups and their use as electron donors for bulk heterojunction solar cells. *RSC Advances*, 3: 18821-18834.
21. Pei, J., Wen, S., Zhou, Y., Dong, Q., Liu, Z., Zhang, J., and Tian, W. (2011). A low band gap donor-acceptor copolymer containing fluorene and benzothiadiazole units: synthesis and photovoltaic properties. *New Journal of Chemistry*, 35: 385-393.
22. Nguyen, T. Q., Yee, R. Y., and Schwartz, B. J. (2001). Solution processing of conjugated polymers: the effects of polymer solubility on the morphology and electronic properties of semiconducting polymer films. *Journal of Photochemistry and Photobiology A: Chemistry*, 144: 21-30.
23. Blouin, N., Michaud, A., Gendron, D., Wakim, S., Blair, E., Neagu-Plesu, R., Belletête, M., Durocher, G., Tao, Y., and Leclerc, M. (2008) Toward a rational design of poly(2,7-carbazole) derivatives for solar cells. *Journal of the American Chemical Society*, 130:732-742.
24. Reyes-Reyes, M., Kim, K., and Carroll, D. L. (2005). High-efficiency photovoltaic devices based on annealed poly(3-hexylthiophene) and 1-(3-methoxycarbonyl)-propyl-1- phenyl-(6,6)<sub>C61</sub> blends. *Applied Physics Letters*, 87(8): 083506-083506-3.
25. Moet, D. J. D., Koster, L. J. A., De Boer, B., and Blom, P. W. M. (2007). Hybrid Polymer Solar Cells from Highly Reactive Diethylzinc: MDMO–PPV versus P3HT. *Chemistry Materials*, 19: 5856-5861.
26. Lee, J.-Y., Shin, W.-S., Haw, J.-R., and Moon, D.-K. (2009). Low band-gap polymers based on quinoxaline derivatives and fused thiophene as donor materials for high efficiency bulk-heterojunction photovoltaic cells. *Journal of Materials Chemistry*, 19: 4938-4945.
27. Yu, D., Yang, Y., Durstock, M., Baek, J.-B., and Dai, L. (2010). Soluble P3HT-Grafted Graphene for Efficient Bilayer–Heterojunction Photovoltaic Devices. *ACS Nano*, 4, 5633-5640.
28. Yi, H., Al-Faifi, S., Iraqi, A., Watters, D. C., Kingsley, J., and Lidzey, D. G. (2011). Carbazole and thienyl benzo[1,2,5]thiadiazole based polymers with improved open circuit voltages and processability for application in solar cells. *Journal of Materials Chemistry*, 21: 13649-13656.
29. Wang, T., Pearson, A. J., Dunbar, A. D. F., Staniec, P. A., Watters, D. C., Yi, H., Ryan, A. J., Jones, R. A. L., Iraqi, A., and Lidzey, D. G. (2012) Correlating Structure with Function in Thermally Annealed PCDTBT:PC70BM Photovoltaic Blends. *Advanced Functional Materials*, 22: 1399-1408.
30. Staniec, P. A., Parnell, A. J., Dunbar, A. D. F., Yi, H., Pearson, A. J., Wang, T., Hopkinson, P. E., Kinane, C., Dalgliesh, R. M., Donald, A. M., Ryan, A. J., Iraqi, A., Jones, R. A. L., and Lidzey, D. G. (2011). The Nanoscale Morphology of a PCDTBT:PCBM Photovoltaic Blend. *Advanced Energy Materials*, 1: 499-504.
31. Pickup, D., Yi, H., and Iraqi, A. (2009). Preparation and properties of alternating 2,7-linked carbazole copolymers with phenylene units with varying number of fluorine substituents. *Journal of Materials Science*, 44: 3172-3178.

32. Kun, H., Yi, H., Johnson, R. G., and Iraqi, A. (2008). Fluoro-protected carbazole main-chain polymers as a new class of stable blue emitting polymers. *Polymers for Advanced Technologies*, 19: 299-307.
33. Sun, Y., Lin, B., Yang, H., and Gong, X. (2012). Improved bulk-heterojunction polymer solar cell performance through optimization of the linker group in donor-acceptor conjugated polymer. *Polymer*, 53: 1535-1542.
34. Lee, W. S., Park, J. H., Baek, M.-J., Lee, Y.-S., Lee, S.-H., Pyo, M., and Zong, K. (2010). Highly efficient synthesis of thieno[3,4-b]thiophene derivatives and (opto)electrochemical properties of new low bandgap conjugated polymers. *Synthetic Metals*, 160: 1368-1371.
35. Abd El Haleem, S. M. and Ateya, B. G. (1981). Cyclic voltammetry of copper in sodium hydroxide solutions. *Journal of Electroanalytical Chemistry and Interfacial Electrochemistry*, 117: 309-319.